AIP | Review of Scientific Instruments

A compact, low cost Marx bank for generating capillary discharge plasmas

A. E. Dyson, C. Thornton, and S. M. Hooker

Citation: Review of Scientific Instruments **87**, 093302 (2016); doi: 10.1063/1.4961913
View online: http://dx.doi.org/10.1063/1.4961913
View Table of Contents: http://scitation.aip.org/content/aip/journal/rsi/87/9?ver=pdfcov
Published by the AIP Publishing

A compact, low cost Marx bank for generating capillary discharge plasmas

A. E. Dyson, C. Thornton, and S. M. Hooker
Department of Physics and John Adams Institute for Accelerator Science, University of Oxford, Denys Wilkinson Building, Keble Road, Oxford OX1 3RH, United Kingdom

(Received 16 March 2016; accepted 17 August 2016; published online 9 September 2016)

We describe in detail a low power Compact Marx Bank (CMB) circuit that can provide 20 kV, 500 A pulses of approximately 100–200 ns duration. One application is the generation of capillary discharge plasmas of density $\approx 10^{18}$ cm^{-3} used in laser plasma accelerators. The CMB is triggered with a high speed solid state switch and gives a high voltage output pulse with a ns scale rise time into a 50 Ω load (coaxial cable) with <4 ns voltage jitter. Its small size (10 cm × 25 cm × 5 cm) means that it can be placed right next to the capillary discharge in the target chamber to avoid the need to impedance match. The electrical energy required per discharge is <1 J, and the CMB can be run at shot repetition rates of ≳1 Hz. This low power requirement means that the circuit can easily be powered by a small lead acid battery and, therefore, can be floated relative to laboratory earth. The CMB is readily scalable and pulses >45 kV are demonstrated in air discharges. *Published by AIP Publishing.* [http://dx.doi.org/10.1063/1.4961913]

I. INTRODUCTION

The gas-filled capillary discharge waveguide (CDW) has been used by several groups to guide high-intensity laser pulses over many Rayleigh ranges.[1] It has found applications in extending the gain length of longitudinally pumped soft X-ray lasers, increasing the X-ray output by nearly an order of magnitude,[2] and in extending the acceleration length of laser-plasma accelerators (LPA's), enabling the generation of electron beams with energies up to 4.2 GeV.[3–6]

The capillary within a CDW is laser-machined[7] into sapphire plates and typically has a diameter of 100–400 μm and a length of several cm. Gas, usually hydrogen, is introduced near each end of the capillary via gas feed lines that are also laser-machined into the sapphire plates. The gas is ionized and heated by a discharge pulse with a peak current of order 200–500 A and a duration of approximately $\tau_p \approx$ 100–200 ns. The discharge plasma is cooled by the capillary walls and so forms a transverse density profile with a minimum on axis, since the pressure across the capillary is nearly constant.[8,9] The transverse refractive index profile of the plasma therefore decreases with radial distance from the capillary axis, forming a plasma channel which can guide an optical beam in the same way as in a gradient refractive index (GRIN) optical fibre. In practice, the spot size of the lowest-order mode of the plasma channel is a few tens of microns.[10]

A number of ways of making the high voltage (HV) pulse needed to generate the discharge plasma have been reported.[11,12] In all of the methods explored to date, the HV pulse is sent to the capillary at the centre of the chamber using a long coaxial cable and so requires impedance matching to avoid reflections. The discharge circuit previously used by the authors[11] consisted of a HV power supply (Glassman—30 kV, 300 W max.) that charged a HV charging capacitor of 1–2 nF to a typical working voltage of 20 kV. This was switched into a 50 Ω coaxial cable (UR67) connecting the capacitor to the CDW by a thyratron switch (E2V CX1685). The charging capacitor, thyratron, and associated circuitry were housed in a metal "thyratron box" of approximately 50 cm × 30 cm × 50 cm. Due to their large size, both the HV supply and thyratron box had to be located outside the vacuum chamber in which the CDW was housed and hence the connecting coaxial cable was typically 3 m long.

The capillary load impedance changes from open circuit to as low as 10–30 Ω for a fully formed plasma and so presents a variable mismatched load. Breakdown occurs as soon as the voltage pulse arrives at the capillary (typically within a few ns) and as a result the voltage pulse is reflected at both the capillary and at the HV input end of the cable. This gives rise to "current bounce" in the cable resulting in the plasma current changing in a stepwise manner on a time scale of twice the cable transit time $2\tau \approx 30$ ns as the current pulse is reflected back and forth down the cable (see Figure 6). This behaviour is distinct from that of the overall current envelope that is characterised by the usual LCR circuit "current ringing"; our circuits are usually just under damped ($\zeta \lesssim 1$). The discharge plasma follows the faster "current bounce" oscillations, which means that the performance of the CDW can vary on time scales much shorter than the overall discharge duration τ_p: for example, in some LPA's with a CDW, the temporal window for generating high-quality electron beams has been found to be as short as 10 ns.[13] In such cases, this sensitivity to timing causes additional experimental difficulty. Note that the minimum τ_p that can be used is determined by the fact that it takes 50–100 ns to have stable plasma channel formation in the capillary[8] (see Figure 7). Whilst the discharge duration must be at least of this order, it should not be excessively long as the resulting I^2R heating can thermally over-stress the capillary walls leading to increased surface erosion and crack formation in the sapphire plates. The use of a much longer coaxial cable with $2\tau > \tau_p$ would give a single step-like profile

for main discharge current pulse, limited by $I_{max} = 2 \times V/Z_0$ (into a short circuit) with $Z_0 = 50\ \Omega$. For $\tau_p = 100$ ns this requires a coaxial cable of length 10 m ($v = 2 \times 10^8$ m/s, 1 m ≡ 5 ns). However, this technique requires fast on and off switching of the coaxial line, and unless the HV input is impedance matched, then there will still be "current bounce" giving reflected current pulses at later times. This long cable approach has been used elsewhere,[12] but the switching speeds used and the mismatched HV input gave an overall discharge duration of several μs, resulting in very much greater capillary heating. Incidentally, this approach is not possible using the thyratron switch as it cannot be rapidly switched off. The use of the thyratron also means that only negative voltage pulses can be generated.

For typical electrical parameters of $V = 20$ kV and $C = 2$ nF, the electrical energy needed is $W = \frac{1}{2}CV^2 < 1$ J. Thus for shot repetition rates of ≈1 Hz, the time averaged power required from the charging HV supply is <1 W. This suggests that a much smaller, low power compact circuit could be used for our application. It should be mentioned here that next generation CDW drivers working at 1 kHz repetition rates have been developed based on the thyratron.[14] The high repetition rate means that these devices are necessarily high power and so large and require external cooling both of the HV supply and the capillary itself.

II. THE COMPACT MARX BANK (CMB) DESIGN

The Compact Marx Bank (CMB) described here is a low power device and has been designed to be placed right next to the capillary. This essentially eliminates the effects "current bounce" giving a smooth current profile (within the bandwidth limits of our measurement probe/oscilloscope) even when there is an impedance mis-match. The charging capacitors effectively discharge directly into the CDW load giving the usual LCR discharge current profile. The peak current is mainly limited by circuit inductance and the current duration (area) by the total charge stored (the capacitance of the charging capacitors). A further important advantage is that the short distances travelled by the discharge current also mean that the CMB generates considerably less electrical noise than the very much larger current loops that were present in the previous circuit. The CMB can be charged using a 12 V lead acid battery and a miniature EMCO PCB 2.5 kV HV supply. As a result, the discharge can be floated with respect to laboratory earth and this inhibits breakdown to the chamber walls. In addition, because all the HV parts are inside the chamber, it is inherently much safer to use. This system also has the considerable advantage that if multiple capillary accelerator stages are used then the discharge units are sufficiently compact that they can be placed side by side inside the chamber. The polarity of the HV pulses can be either positive or negative depending on the sign of the charging supply. The CMB described here was selected to give positive HV pulses. This was done as it was found that having the HV electrode as an anode, as opposed to a cathode, reduces the likelihood of unwanted discharge to the chamber or nearby optical mounts (i.e., over distances of tens of cm at chamber backing pressures of 10^{-3} mbar). This is because having a negative HV electrode facilitates electron multiplication in the strong cathode fields relative to the weaker field lines terminating on the much larger "electrode" represented by chamber earth.

The CMB assembly is housed in an air-tight box placed inside the vacuum chamber; this box is shown in Figure 1. The box is maintained at atmospheric pressure internally via a plastic tube connected to the outside of the chamber; the air is needed both for the insulation of the HV components and the correct operation of the spark gaps (SG's). The box has SHV (Safe High Voltage) connections for an external trigger pulse and an externally generated charging voltage of up to 2.5 kV (although this could readily be internally generated in the box using an EMCO PCB HV supply). The box consists of a trigger unit and a CMB insert as described below.

A. The CMB insert

A circuit schematic of the CMB insert is given in Figure 2(a). It consists of the usual Marx bank arrangement of an RC ladder network in which the capacitors are charged in parallel and then discharged in series through the SG's. This low cost design uses only capacitors and resistors with the resistor leads acting as the SG's. The number of ladder "rungs" N gives the voltage multiplication factor and the rung capacitance determines the output pulse duration for a given load discharging the capacitors. The charging time can be

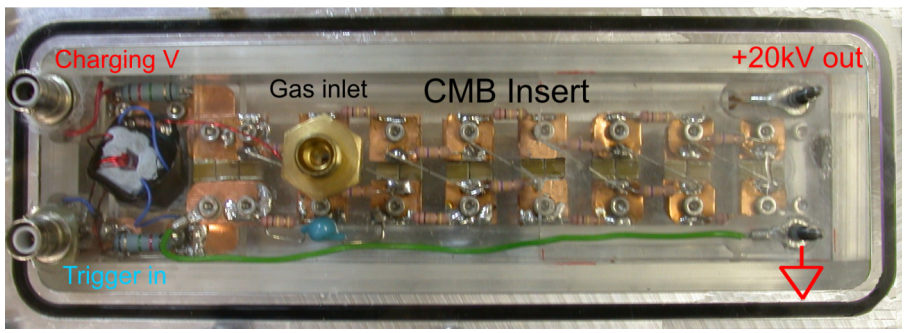

FIG. 1. The air-tight box containing the fixed trigger unit (left 1/5) and the removable CMB insert (right 4/5). This is placed inside the evacuated target chamber close to the CDW. The gas inlet allows a gas line to be connected so that the CMB is maintained at atmospheric pressure to ensure proper operation of the spark gaps. The HV output pins on the right connect to the CDW.

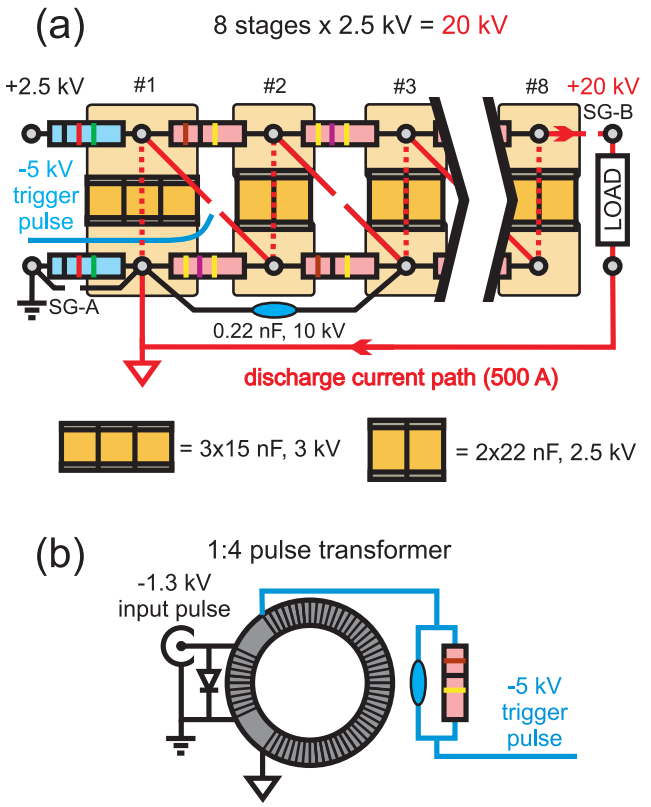

FIG. 2. (a) Schematic of the 8 stage CMB. In addition to the usual Marx bank arrangement, SG-A protects the trigger circuit by isolating the different earths; SG-B isolates the load from the charging voltage. (b) The trigger unit pulse transformer.

roughly estimated from the empirical formula $\tau_c \approx 2N^2RC$ (all R's and C's the same). The CMB shown uses 8×44 nF rungs with alternate 100/470 kΩ metal film HV resistors. These values are chosen to limit the current so that the SG's do not stay open after firing if the charging voltage is constantly applied (if the charging supply is switched then smaller resistor values can be used, see below). The ladder network is isolated from the charging supply using 1.2 MΩ HV resistors on both the charging and "earth" sides. These combined resistor values give a charging time to >95% full voltage of around 2 s for this particular insert. A faster "1 Hz" CMB insert has also been be made by using only 100 kΩ resistors (the smallest value available). This is useful even in LPA experiments, where the high power laser repetition rate is ≪1 Hz as it can also be run in "alignment mode" allowing for faster capillary alignment at low power. However, this does require the use of a switched supply that removes the charging voltage between shots to allow the SG's to reset (requires several ms). Faster repetition rates of ≲10 Hz would be possible by using paralleled resistors (R = 50 kΩ) and smaller rung capacitance (C = 10 nF) but then the charging time τ_c and power dissipation in the 0.5 W resistors are limiting factors. Once SG#1 has been triggered, the subsequent SG's fire due to being overvoltaged and charging the "stray" capacitance of each stage to its surroundings. Since this capacitance is small (typically tens of pF), this results in only very weak sparks (for no load). The side 0.22 nF capacitor sinks much larger current from SG#2 on breakdown greatly improving the "quality" (brightness and shot to shot consistency) of this spark, needed here as this gap is only just overvoltaged. This assistance is not needed higher up the chain where the significant overvoltage due to the ganged lower stages is easily sufficient to cause reliable breakdown.

The compactness of the CMB is made possible by the use of multi-layer ceramic (MLC) chip capacitors (5.7 mm × 6.4 mm × 2.5 mm) of capacitance 22 nF that can be charged to 2.5 kV giving an energy density of >750 mJ/cm^3 (cf. ≈30 mJ/cm^3 for polypropylene capacitors). The design uses the rung resistor leads to form the SG's with the gap set to 1–2 mm. The gaps are adjusted so that the SG's just hold off when charging. It found that the CMB will operate reliably over quite a wide range of supply voltages of 2–2.5 kV giving some control of the erected voltage. The Marx bank is mounted on a thin rectangular perspex sheet to give an insert (160 mm × 40 mm × 10 mm) separate from the trigger unit. This is done so that the insert can be easily changed should one of the capacitors fail, for example due to repeated accidental firing into a short circuit. The width of the insert exceeds that of the CMB circuit by 10 mm on all sides to prevent shorting to the walls at atmospheric pressure. The walls are also further insulated by 10 mm thick perspex sheet cladding. The box has a top window of 15 mm thick perspex sheet to allow observation of the SG's and so confirms correct operation. It is found that the front window does not introduce significant electrical noise into the chamber (for example, motorized mirrors and optomechanical stages were unaffected by electrical noise) and so additional wire mesh shielding was not used.

B. The triggering unit

A schematic of the triggering unit is shown in Figure 2(b). The CMB is triggered using a −5 kV HV trigger pulse that is applied via a hair trigger, a thin wire held in close proximity to SG #1. This HV pulse overvolts SG #1 and so initiates the CMB breakdown. The pulse is generated in the secondary of a pulse transformer that consists of a single ferrite core with 10:40 primary/secondary turns. The external trigger pulse is generated with a high speed MOSFET HV switch that sends a −1.25 kV, 100 ns pulse with <5 ns risetime down a 50 Ω coax. This pulse is fed to the transformer primary via the vacuum box SHV trigger in. It is found that this system gives reliable triggering and also sufficiently isolates the primary circuit from the main CMB.

III. THE CMB ELECTRICAL CHARACTERISTICS

A. Output impedance

The CMB was characterised by firing into a 50 Ω load (either a resistor or a very long UR67 coaxial cable) placed directly at its output. Measurements of the voltage were made using a fast Tektronix P6015 high voltage probe (20 kV/1000x, bandwidth DC—75 MHz) connected to a Tektronix TDS3012B oscilloscope (bandwidth DC—100 MHz). The resulting voltage trace at the CMB output is shown in Figure 3. This shows an apparent slow rise time

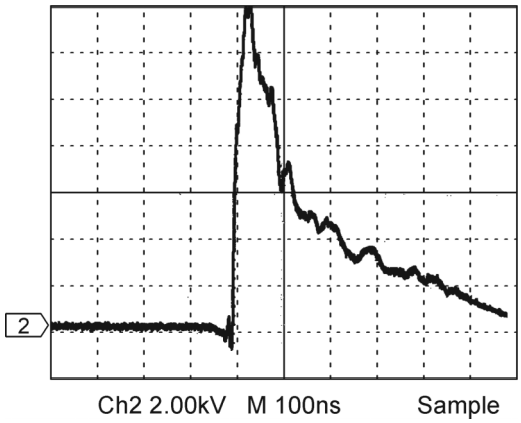

FIG. 3. Oscilloscope screen of the CMB output voltage as a function of time when discharging into a 50 Ω load. The oscilloscope was set to 2 kV/division on the vertical scale and 100 ns/division on the horizontal scale. The CMB was charged to $V_0 = 18$ kV and the load voltage of $V_0 = 14$ kV shows that the CMB output impedance is $Z_0 \approx 10$ Ω.

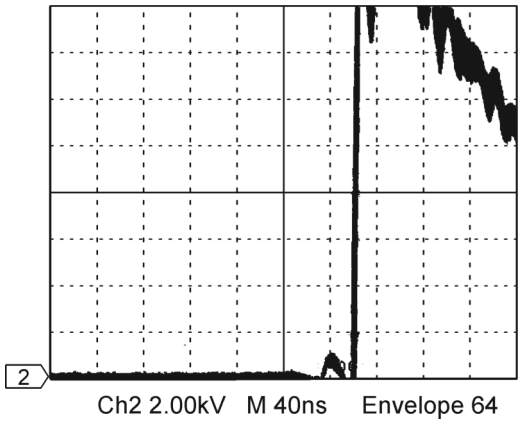

FIG. 4. Oscilloscope screen of the CMB output voltage as a function of time when discharging into a 30 mm CDW with $p = 100$ mbar. The oscilloscope was set to 2 kV/division on the vertical scale and 40 ns/division on the horizontal scale and put in envelope mode. In this mode all traces are overlaid on the screen. The width of the envelope shows that the CMB voltage jitter is around ±4 ns.

of 5 ns, but this measurement is bandwidth limited and so the actual rise time is likely to be much faster. The trace then shows an RC decay with time constant $\tau \approx 200$ ns. This gives a measured erected $C \approx 4$ nF compared to an expected value of $C = 44/8 = 5.5$ nF (rung capacitors now in series). The CMB was charged to give an output $V = 18$ kV and the measured output voltage into 50 Ω is $V_0 = 14$ kV. Using $V_0/V = 50/(Z_0 + 50)$ indicates that the CMB has an apparent output impedance $Z_0 \approx 10$ Ω when driving a 50 Ω load. This is due to SG losses and the effects of stray capacitance.

B. Pulse jitter

In LPA applications using the CDW the discharge must be synchronized to the laser pulse to be guided. Results obtained using the previous external HV circuit (with "current bounce") suggested that the jitter between the CDW trigger (derived from the laser trigger system) and the discharge current needed to be less than 10 ns. The smooth current profile of the CMB is found to considerably relax this requirement, see Section IV. The CMB pulse jitter was measured using CDW's with diameter 300 μm and a range of lengths L from 15 mm to 100 mm. The voltage jitter measurements for a 30 mm CDW at $p = 100$ mbar are typical and shown in Figure 4. This figure shows the oscilloscope screen with the oscilloscope in "envelope" mode. In this mode, all the captured traces are overlaid on top of each other so that any variation between shots is clearly visible. Since this gives an envelope trace bounded by the "outliers," our jitter values are for "envelope" jitter and give a rough estimate of the range that around 95% of shots are likely to fall within (2σ). These measurements give an estimated envelope voltage jitter of ±3–4 ns.

For a CDW, the current jitter is expected to be larger than the voltage jitter due to the stochastic nature of the plasma avalanche breakdown process. Moreover, special care must be taken with the design of the hollow Cu electrodes that are placed either side of the capillary. This is because the expanding gas plumes exiting the capillary into vacuum must have good "contact" with the electrodes otherwise the onset of breakdown is significantly impeded. This becomes increasingly important for low fill pressures $p < 50$ mbar, the working pressure range of the longer CDW's. For this reason, Cu washers with a central hole just larger than the capillary were sandwiched between the sapphire plate ends and the electrodes. The discharge current jitter was measured using a Pearson current monitor Model 410 (bandwidth 120 Hz-20 MHz) placed at the plasma load. Typical tests on a 30 mm CDW at $p = 100$ mbar give current jitter value of around ±6 ns. It is found that the current jitter increases slightly with increasing L but increases much more with decreasing p, the main impediment to breakdown not being added length but low gas pressure around the electrodes. The 8 rung CMB used here can drive a 100 mm CDW operating at $p = 30$ mbar but with an increased current jitter of around ±15 ns. This jitter would be significantly reduced by using a slightly higher discharge voltage as we are operating only a few kV above to the minimum voltage needed for breakdown. Thus for the 100 mm CDW, a 10 rung CMB would be better, each additional rung adding 2 cm to the length of the insert.

C. CMB insert reliability/lifetime

For this very simple, very compact unit, we have chosen to use SG's as no existing single package solid state switch is able to handle this combination of high voltage and high current with ns time scale risetimes. This means that an occasional mis-fire will occur as the SG's are tuned close to their hold off limit in order to get low jitter. In order to establish the reliability and lifetime of the CMB, the circuit was repetitively fired into a 50 Ω load for many thousands of shots with the oscilloscope left in envelope mode. It was found that the slower, non-switched CMB when triggered at 0.5 Hz misfires less than once every 1500–2500 shots, usually self-breakdown just before the trigger. This occurs because the SG's have to hold off the maximum voltage for some time

thus increasing the chance of self-breakdown. This unwanted behaviour can be minimised by using a pre-triggered relay to switch the charging voltage on just long enough for the CMB to charge up before the main shot trigger arrives. The "1 Hz" CMB trigged at 1 Hz can run for >3 h of operation without a misfire. Here the charging voltage was switched on for 0.95 s with an off time of 0.05 s between shots to allow the SG's to reset.

The 2×22 nF rung capacitors in the CMB insert can only repetitively handle up to 500 A, and at 150% of this current, the lifetime falls to hundreds of shots before one of the capacitors fails. In order to protect the capacitors, extra long thin connecting leads (length 30 cm, SWG 15) were used between the CMB and the discharge so that the increased circuit inductance limited the maximum current in the case of accidental short circuit.

The SG resistor leads, when placed tip to tip, were seen to erode due to repetitive use over many thousands of shots, thus gradually increasing the gap distance. This was found to result in unreliable operation (around one in 1000 shots misfires) after >10 000–15 000 shots. The CMB insert then has to be removed and the SG's regapped. This erosion of the gaps can be significantly reduced by placing the resistor leads side by side, in parallel, with an overlap length of around 1 cm and this greatly increases the gap lifetime. This also significantly reduces the internal circuit inductance. However, the tip to tip arrangement used here is preferred for ease of tuning (gap setting to optimise jitter).

IV. CAPILLARY DISCHARGE PLASMAS

The plasma produced by the CMB is shown in Figure 5. The channel is found to be uniformly illuminated along its full length and this gives some indication of uniform plasma generation. The discharge current driven in the CDW at $p = 100$ mbar by the CMB and, for comparison, by the external HV circuit with a 3 m coaxial cable is shown in Figure 6. The "current bounce" produced by the external circuit is clearly seen with a time scale of twice the cable transit time $2\tau = 30$ ns. By contrast that produced by the CMB has a smooth profile and this allows the plasma guiding channel to evolve in a consistent manner. This is found that this greatly increases the laser pulse guiding window.

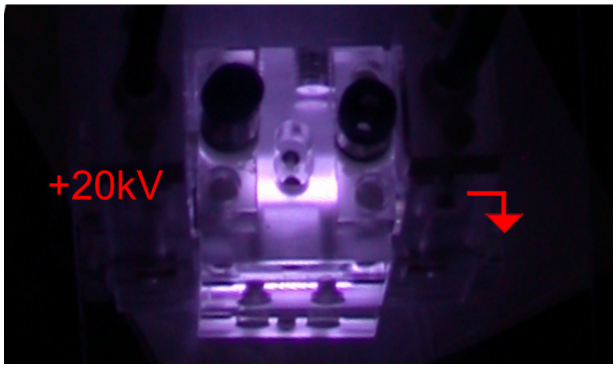

FIG. 5. The capillary discharge plasma, magnified by the sapphire capillary block ($L = 30$ mm). The HV feed cables are shown on the left side (20 kV) and right side (Earth) of the capillary and connect to Cu annular electrodes.

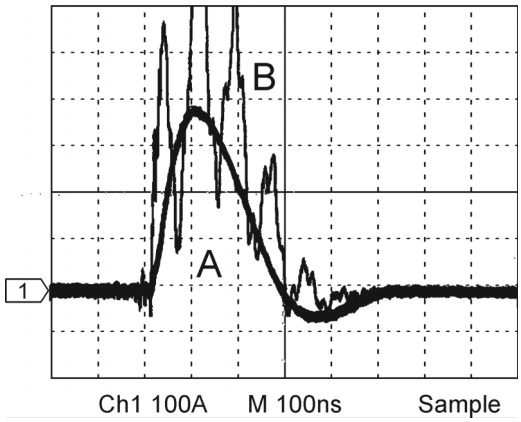

FIG. 6. Oscilloscope screen of the discharge current as a function of time for a 30 mm CDW with $p = 100$ mbar. The oscilloscope was set to 100 A/division on the vertical scale and 100 ns/division on the horizontal scale. Trace A is for the CMB placed next to the capillary showing a smooth current profile. Trace B is for an external HV circuit connected to the capillary using a 3 m coaxial cable and clearly shows "current bounce."

The CMB forms an LCR circuit with the resistive/inductive plasma load. The current profile is determined by (V, L, C, R), the CMB voltage, circuit inductance, CMB capacitance, and plasma resistance, respectively. The current profile shown is under damped and taking $V \approx 15$ kV, $C \approx 5$ nF (known) gives values of $R \approx 25\ \Omega$ and $L \approx 2\ \mu$H. Not all of the (V, L, C, R) can be varied since for the CDW then $V \approx 15$ kV (for breakdown) and $R \approx 25\ \Omega$ (plasma resistance). We can vary C with the present CMB design to around 1–10 nF and also add circuit L (to the contributions of the CMB and CDW). An external series R can be added since before breakdown the CDW has $R = \infty$ and so the full HV will appear across it. For example, it has been shown that stable guiding can occur for currents as low as 50 A.[14] If the peak current is reduced here by adding a large series L and reducing C then the result is a very underdamped circuit with considerable current ringing and so resistive damping is needed. Full control of both the peak current and the current profile is not always possible with the CMB in a simple LCR circuit configuration.

Interferometric measurements of capillary discharges driven by the CMB were undertaken to confirm that they generated plasma channels suitable for guiding high-intensity laser pulses. The measurements were performed using a 30 mm CDW of square cross section with side $a = 150\ \mu$m, placed in one arm of a Mach-Zehnder interferometer illuminated by 1064 nm and 532 nm (2ω) probe pulses of less than 10 ns duration from a Nd:YAG laser. A dielectric mirror directed the two beams to separate CCD cameras, and interferograms were recorded as a function of the delay t between the start of the discharge current and the arrival of the probe laser pulses. As described in our earlier work,[10] the simultaneous two-colour interferometry allowed phase shifts other than those introduced by the plasma electrons to be detected and accounted for.

Figure 7 shows the deduced transverse electron density profiles at several delays t. It can be seen that the on-axis

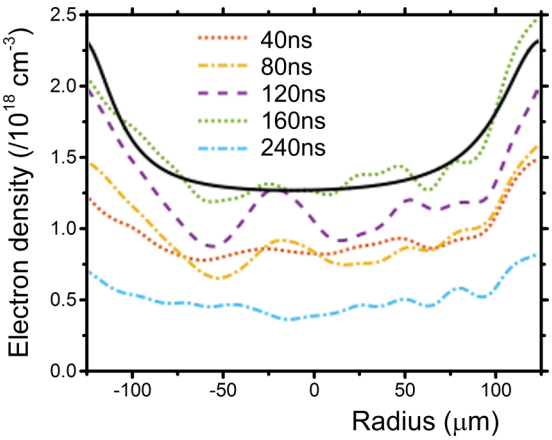

FIG. 7. Interferometric measurements of the electron density as a function of transverse position in a CDW of square cross section driven by the CMB. Results are shown for various delays t between the start of the discharge current and the arrival of the probe laser pulses, as indicated in the legend. The solid black line shows a fit to the data for $t = 160$ ns.

electron density profile increases until shortly after the peak of the discharge current, thereafter returning close to zero in approximately 60 ns. The plasma develops a distinct well of depth Δn_e which increases until close to the peak of the discharge current at which time $\Delta n_e \approx 0.8 \times 10^{18}$ cm^{-3}. The matched spot size w_M of the lowest-order mode of a plasma channel is largely independent of the shape of the electron density profile[10] and is given by the smallest radius $r = w_M$ for which the increase in the electron density above the axial value is $\Delta n_e = (\pi r_e r^2)^{-1}$, where $r_e = e^2/mc^2$ is the classical electron radius. Our results suggest $w_M \approx 33$ μm, which is close to the value of $w_M \approx 36$ μm predicted by previously determined scaling laws.[10] These interferometric measurements show that the plasma channel produced with the CMB circuit is suitable for guiding from $t = 60$–200 ns, i.e., a guiding window of about 140 ns. This has been confirmed in LPA experiments both directly by observing the laser guiding and indirectly from the fact that enhanced accelerated self-injection electron production only occurs over this range. This very considerably simplifies the experimental task of timing the discharge.

The CMB concept is readily scalable to higher voltages by using more RC ladder rungs. To test that this is practicable a 20 rung CMB was built. This gave a >45 kV pulse (charging voltage 2.3 kV) resulting in air discharge over a gap of $L = 40$ mm as shown in Figure 8.

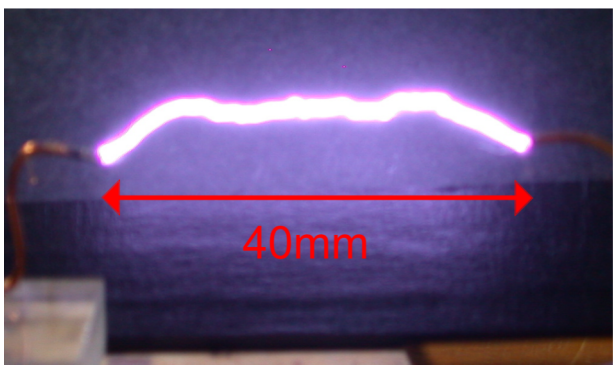

FIG. 8. Arc struck in air over a 40 mm gap to show a >45 kV CMB discharge. This CMB uses 20 ladder rungs with $R = 100$ kΩ and $C = 15$ nF each charged to 2.3 kV (breakdown voltage in air ≈ 10 kV/cm).

V. SUMMARY

We have developed a low power compact Marx bank (CMB) that can generate high voltage pulses of >45 kV, with currents up to 500 A of around 100–200 ns duration. The low cost design uses only capacitors and resistors with the resistor leads acting as the spark gaps (SG's). An 8 rung CMB has been operated at pulse repetition rates of $\gtrsim$1 Hz. This low repetition rate allows it to be powered by a small lead acid battery and miniature low power 2.5 kV HV supply. One application is driving the capillary discharge waveguide (CDW) for laser plasma accelerators (LPA's). This CMB generates up to 20 kV with peak currents of 250–400 A when driving the CDW with a just under damped current profile. The peak current is limited by circuit inductance and the discharge duration by the CMB capacitance. The CMB is designed to be placed inside the target chamber, right next to the CDW, so eliminating the need for impedance matching as the cable transit time is negligible. This avoids the "current bounce" that is present with mismatched externally driven discharges that have to use long coaxial cables to reach the capillary. The CMB's smooth current profile is highly advantageous, since it increases the timing window for guiding from 10 ns (due to "current bounce" that affects the waveguide behaviour) to around 140 ns. For this very simple, very compact unit we have chosen to use SG's as no existing single package solid state switch is able to handle this combination of high voltage and high current with ns time scale risetimes. This means that an occasional misfire is inherent in this technology and the CMB inserts have to be regapped due to SG erosion. The compactness of the CMB means that many units can be placed next to each other in LPA's that require staging.

ACKNOWLEDGMENTS

This work was supported by the Science and Technology Facilities Council (Grant No. ST/J002011/1).

[1]A. Butler, D. J. Spence, and S. M. Hooker, Phys. Rev. Lett. **89**, 185003 (2002).
[2]A. Butler, A. J. Gonsalves, C. M. McKenna, D. J. Spence, S. M. Hooker, S. Sebban, T. Mocek, I. Bettaibi, and B. Cros, Phys. Rev. Lett. **91**, 205001 (2003).
[3]W. P. Leemans, B. Nagler, A. J. Gonsalves, C. S. Tóth, K. Nakamura, C. G. R. Geddes, E. Esarey, C. B. Schroeder, and S. M. Hooker, Nat. Phys. **2**, 696 (2006).
[4]S. Karsch, J. Osterhoff, A. Popp, T. P. Rowlands-Rees, Z. Major, M. Fuchs, B. Marx, R. Horlein, K. Schmid, L. Veisz, S. Becker, U. Schramm, B. Hidding, G. Pretzler, D. Habs, F. Gruner, F. Krausz, and S. M. Hooker, New J. Phys. **9**, 415 (2007).
[5]T. P. A. Ibbotson, N. Bourgeois, T. P. Rowlands-Rees, L. S. Caballero, S. I. Bajlekov, P. A. Walker, S. Kneip, S. P. D. Mangles, S. R. Nagel, C. A. J. Palmer, N. Delerue, G. Doucas, D. Urner, O. Chekhlov, R. J. Clarke, E. Divall, K. Ertel, P. S. Foster, S. J. Hawkes, C. J. Hooker, B. Parry, P. P. Rajeev, M. J. V. Streeter, and S. M. Hooker, Phys. Rev. Spec. Top.–Accel. Beams **13**, 031301 (2010).
[6]W. P. Leemans, A. J. Gonsalves, H. S. Mao, K. Nakamura, C. Benedetti, C. B. Schroeder, C. Toth, J. Daniels, D. E. Mittelberger, S. S. Bulanov, J. L. Vay, C. G. R. Geddes, and E. Esarey, Phys. Rev. Lett. **113**, 245002 (2014).

[7]S. M. Wiggins, M. P. Reijnders, S. Abuazoum, K. Hart, G. H. Welsh, R. C. Issac, D. R. Jones, and D. A. Jaroszynski, Rev. Sci. Instrum. **82**, 096104 (2011).
[8]N. A. Bobrova, A. A. Esaulov, J. I. Sakai, P. V. Sasorov, D. J. Spence, A. Butler, S. M. Hooker, and S. V. Bulanov, Phys. Rev. E **65**, 016407 (2002).
[9]B. Broks, K. Garloff, and J. van der Mullen, Phys. Rev. E **71**, 016401 (2005).
[10]A. J. Gonsalves, T. P. Rowlands-Rees, B. H. P. Broks, J. J. A. M. van der Mullen, and S. M. Hooker, Phys. Rev. Lett. **98**, 025002 (2007).
[11]D. J. Spence and S. M. Hooker, Phys. Rev. E **63**, 015401 (2000).
[12]S. Abuazoum, S. M. Wiggins, R. C. Issac, G. H. Welsh, G. Vieux, M. Ganciu, and D. A. Jaroszynski, Rev. Sci. Instrum. **82**, 063505 (2011).
[13]T. P. A. Ibbotson, N. Bourgeois, T. P. Rowlands-Rees, L. S. Caballero, S. I. Bajlekov, P. A. Walker, S. Kneip, S. P. D. Mangles, S. R. Nagel, C. A. J. Palmer, N. Delerue, G. Doucas, D. Urner, O. Chekhlov, R. J. Clarke, E. Divall, K. Ertel, P. Foster, S. J. Hawkes, C. J. Hooker, B. Parry, P. P. Rajeev, M. J. V. Streeter, and S. M. Hooker, New J. Phys. **12**, 045008 (2010).
[14]A. J. Gonsalves, F. Liu, N. A. Bobrova, P. V. Sasorov, C. Pieronek, J. Daniels, S. Antipov, J. E. Butler, S. S. Bulanov, W. L. Waldron, D. E. Mittelberger, and W. P. Leemans, J. Appl. Phys. **119**, 033302 (2016).